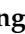





Article

Characterization of Microbial Communities Associated with Ceramic Raw Materials as Potential Contributors for the Improvement of Ceramic Rheological Properties

Angela M. Garcia-Sanchez ¹, Bernardino Machado-Moreira ², Mário Freire ³, Ricardo Santos ³, Sílvia Monteiro ³, Diamantino Dias ⁴, Orquídia Neves ², Amélia Dionísio ² and Ana Z. Miller ^{5,6,*}

¹ Department of Microbiology and Parasitology, Faculty of Pharmacy, University of Seville, Profesor García González 2, 41012 Seville, Spain; agarcia77@us.es

² CERENA, Instituto Superior Técnico, Universidade de Lisboa, Av. Rovisco Pais 1, 1049-001 Lisboa, Portugal; bernardinommoreira@gmail.com (B.M.-M.); orquidia.neves@tecnico.ulisboa.pt (O.N.); amelia.dionisio@tecnico.ulisboa.pt (A.D.)

³ Laboratorio de Análises do Instituto Superior Técnico, Universidade de Lisboa, Av. Rovisco Pais 1, 1049-001 Lisboa, Portugal; mario.freire@tecnico.ulisboa.pt (M.F.); ricardosantos@tecnico.ulisboa.pt (R.S.); silvia.monteiro@tecnico.ulisboa.pt (S.M.)

⁴ Rauschert Portuguesa, SA., Estrada Nacional 249-4, Trajouce, 2785-653 São Domingos de Rana, Portugal; diamantinodias@rauschert.pt

⁵ Instituto de Recursos Naturales y Agrobiología de Sevilla (IRNAS-CSIC), Av. Reina Mercedes 10, 41012 Sevilla, Spain

⁶ HERCULES Laboratory, University of Évora, Largo Marquês de Marialva 8, 7000-809 Évora, Portugal

* Correspondence: anamiller@irnas.csic.es; Tel.: +34-954-624-711

Received: 29 March 2019; Accepted: 20 May 2019; Published: 23 May 2019



Abstract: Technical ceramics are being widely employed in the electric power, medical and engineering industries because of their thermal and mechanical properties, as well as their high resistance qualities. The manufacture of technical ceramic components involves complex processes, including milling and stirring of raw materials in aqueous solutions, spray drying and dry pressing. In general, the spray-dried powders exhibit an important degree of variability in their performance when subjected to dry-pressing, which affects the efficiency of the manufacturing process. Commercial additives, such as deflocculants, biocides, antifoam agents, binders, lubricants and plasticizers are thus applied to ceramic slips. Several bacterial and fungal species naturally occurring in ceramic raw materials, such as *Sphingomonas*, *Aspergillus* and *Aureobasidium*, are known to produce exopolysaccharides. These extracellular polymeric substances (EPS) may confer unique and potentially interesting properties on ceramic slips, including viscosity control, gelation, and flocculation. In this study, the microbial communities present in clay raw materials were identified by both culture methods and DNA-based analyses to select potential EPS producers based on the scientific literature for further assays based on the use of EPS for enhancing the performance of technical ceramics. Potential exopolysaccharide producers were identified in all samples, such as *Sphingomonas* sp., *Pseudomonas xanthomarina*, *P. stutzeri*, *P. koreensis*, *Acinetobacter lwoffii*, *Bacillus altitudinis* and *Micrococcus luteus*, among bacteria. Five fungi (*Penicillium citrinum*, *Aspergillus niger*, *Fusarium oxysporum*, *Acremonium persicinum* and *Rhodotorula mucilaginosa*) were also identified as potential EPS producers.

Keywords: ceramic raw materials; industry; additives; EPS; bacteria; fungi

1. Introduction

The ceramic industry represents an important sector of economic activity in the European countries. Technical ceramics in particular, also called high-performance ceramics, are being widely employed in the electric power, medical and engineering industries due to their thermal, mechanical properties and high resistance qualities. Technical ceramic components can be manufactured by different processes, such as unidirectional dry pressing, extrusion, isostatic pressing and injection molding [1]. Considering the unidirectional dry pressing, this method involves the milling and stirring of the raw materials in aqueous suspensions (slips), followed by spray-drying of the slip to remove the water excess, and obtain a fine powder that is further subjected to unidirectional dry pressing (conformation). In general, the resulting spray-dried powders exhibit an important degree of variability in their performance, specifically during conformation, due to the adhesion of the conformed part to the mold, and the different mechanical strength of the conformed ceramic product. This variability affects the efficiency of the manufacturing process. To overcome this drawback, several commercially available organic additives are employed. Deflocculants, biocides, antifoam agents, binders, lubricants and plasticizers are added into ceramic slips to achieve homogeneous and uniform pastes, modelling the rheological properties of the ceramic slips. Nevertheless, some of the employed additives are toxic for human health, and their application also represents an increase in the cost of the manufacturing process. Thus, scientific knowledge in this area plays a fundamental role in defining new strategies and new sustainable and cost-effective procedures to improve the efficiency of industrial ceramic production.

Several microorganisms are known for their ability to synthesize and excrete exopolysaccharides or extracellular polymeric substances (EPS) for surviving and adhering to solid surfaces [2]. Because of their physical and rheological properties, these polymers confer potentially interesting applications to the industrial sector [3,4]. Many EPS, such as xanthan, alginate, dextran, pullulan and glucan, have a wide range of applications in food, pharmaceutical, biomedical, petroleum, and other industries [5–7]. Some properties of EPS should be considered of high interest for the technical ceramics industry to improve the rheological properties of the slips and to decrease the difficulties observed during the unidirectional dry pressing process. In addition, the application of EPS may reduce production costs and the environmental impact caused by some commercial additives. Ceramic raw materials, such as talc and bentonite, naturally contain bacteria and fungi. It is thus of utmost interest to characterize the microbial diversity present in such materials to further assess their EPS production capacity with useful properties for the industrial ceramic sector.

This work is focused on the identification of microbial communities associated with ceramic raw materials and slips used at the technical ceramic producer, Rauschert Portuguesa S.A., Portugal (hereinafter Rauschert Portuguesa) in order to highlight EPS producers that may have industrial and/or commercial potential based on the literature.

2. Materials and Methods

2.1. Sampling

Samples were collected at Rauschert Portuguesa, a leading manufacturer of technical ceramics in Portugal. Samples were collected during the manufacturing process of one of the main types of ceramic produced in the plant by unidirectional dry pressing. The ceramic formulation was a steatite, and it was chosen due to its importance in commercial terms to the manufacturing plant. This formulation is mainly composed of different raw materials, comprising talcs, clay, bentonite and barium carbonate, as confirmed by FTIR analysis (see Section 3.1). Samples of raw materials and ceramic suspensions (Table 1) were collected aseptically from individual transportation bags into 50 mL sterile containers (Figure 1A,B). Three replicates were collected from each ceramic raw material and slips (Figure 1C). At the laboratory, approximately 20 g of each replicate were combined and homogenized under aseptic conditions and further used for culture-dependent techniques and

molecular biology analyses. Subsamples for culture methods were immediately processed, and those intended for molecular biology analysis were kept at $-80\text{ }^{\circ}\text{C}$ until processing.

Table 1. Description and characteristics of studied samples.

Sample ID	Sample Description	Source
1A	Ceramic suspension collected from the mill used to mix and mill all the raw materials with water	Rauschert Portuguesa SA.
2B	Talc 1 collected from individual packing bag *	Rauschert Portuguesa SA.
3C	Talc 2 collected from individual packing bag *	Rauschert Portuguesa SA.
4D	Clay collected from individual packing bag *	Rauschert Portuguesa SA.
5E	Bentonite collected from individual packing bag *	Rauschert Portuguesa SA.
6F	Barium carbonate collected from individual packing bag *	Rauschert Portuguesa SA.
7G	Talc 3 collected from individual packing bag *	Rauschert Portuguesa SA.
8H	Ceramic suspension collected from a mixing tank used to prepare the ceramic slip for further spray-drying	Rauschert Portuguesa SA.

* Due to intellectual property protection, the suppliers of the ceramic raw materials are not mentioned.



Figure 1. Sampling at Rauschert Portuguesa of ceramic raw materials and slips: (A) sampling of talc into sterile containers; (B) clay minerals collection from transportation bag; (C) replicates collected from each raw material; (D) ceramic slip from the mixing tank was collected directly into sterile containers.

2.2. Mineralogical Characterization by FTIR

Ceramic raw materials collected at Rauschert Portuguesa were characterized by Fourier-transform infrared spectroscopy (FTIR). FTIR spectra were recorded with a Perkin Elmer Spectrum 65 spectrometer (PerkinElmer, Waltham, MA, USA) for samples dried at $70\text{ }^{\circ}\text{C}$ to eliminate the effect of water molecules. Powdered samples were dispersed in KBr pellets and IR spectra were recorded for the 4000 cm^{-1} to 400 cm^{-1} region. A total of 128 scans were recorded, with a resolution of 4 cm^{-1} .

2.3. Identification of Microorganisms by Culture Methods

Culture-dependent techniques were carried out for the isolation and identification of potential EPS producers. Therefore, 5 g of each sample was eluted in 25 mL of sterile water. Subsequently, 100 μL of each sample suspension was inoculated on R2A (Reasoner's 2A agar), 10 \times dilute R2A, NA (Nutrient Agar) and 10 \times dilute NA culture media, and plates were incubated at $25\text{ }^{\circ}\text{C}$ for 12 days. Bacteria were isolated on the same culture media, based on their morphology. Fungi were isolated on Sabouraud Dextrose Agar (SDA) culture medium and incubated at $22\text{ }^{\circ}\text{C}$ until fungal growth was obtained. For the identification of fungi, colony characteristics in the culture plate were first assessed, followed by light microscopy examination of the fungal structures stained with lactophenol blue solution (Fluka, France).

Bacterial isolates were identified by DNA-based analyses. DNA from bacterial isolates was extracted with GenoLyse kit (Bruker), according to the manufacturer's instructions. PCR amplification of bacterial 16S rRNA gene was performed using the primer pair 27F (5'AGAGTTTGTATYMTGGCTCAG-3') [8] and 907R (5'CCCCGTCAATTCATTTGAGTTT-3') [9] with the following PCR conditions: a 2 min denaturation step at $94\text{ }^{\circ}\text{C}$, followed by 30 cycles of denaturation

(15 s at 94 °C), annealing (15 s at 55 °C) and elongation (2 min at 72 °C), with a terminal elongation step of 10 min at 72 °C. PCR products were analyzed in 1% (w/v) agarose gels. The DNA fragments with positive signal were sequenced by Macrogen Europe Sequencing Services (Amsterdam, The Netherlands) using the universal bacterial primer 27F.

The sequences of isolated microorganisms obtained in this study were deposited in GenBank under accession numbers LR536330–LR536365.

2.4. Identification of Microorganisms by Molecular Biology Techniques

2.4.1. DNA Extraction and PCR Amplification

DNA from a composite sample of each ceramic raw material (~500 mg) was extracted using the FastDNA Spin Kit for Soil (MP Biomedicals), according to the manufacturer's instructions, and quantified using a Qubit 2.0 fluorometer (Invitrogen, Carlsbad, CA, USA). PCR amplification of bacterial 16S rRNA gene was performed using the primer pair 27F and 907R, as described in Section 2.2. PCR amplification of the fungal ITS regions was performed using the primer pair ITS5 (5'-GAAGTAAAAGTCGTAACAAGG-3') and ITS4 (5'-TCCTCCGCTTATTGATATGC-3') [10] with the following PCR conditions: a 2 min denaturation step at 94 °C, followed by 35 cycles of denaturation (15 s at 94 °C), annealing (1 min at 50 °C) and elongation (1 min at 72 °C), followed by a final step of elongation of 5 min at 72 °C. The PCR reaction mixture (1 mL) consisted of 775 µL of sterile ultrapure water, 200 µL of PCR buffer (MyTaq™ DNA Polymerase, BIOLINE), 5 µL of Taq polymerase buffer (MyTaq™ DNA Polymerase, BIOLINE) and 10 µL of each primer (50 mM). PCR reactions were performed in 0.2 mL PCR tubes containing 25 or 50 µL of reaction mixture and from 0.5 to 2 µL of DNA template (pure or diluted to 2 ng/µL). All PCR products were inspected in 1% (w/v) agarose gels.

2.4.2. Clone Library Construction

In order to obtain 16S rDNA and ITS sequence information of the major bacterial and fungal members comprising the ceramic samples from Rauschert Portuguesa, clone libraries were constructed by cloning PCR products amplified with 27F-907R and ITS5-ITS4 primer pairs. Before cloning, PCR products were purified using the JetQuick PCR Purification Spin Kit (Genomed, Löhne, Germany) according to the manufacturer's protocol, in order to remove primers, dNTPs and enzyme.

DNA clone libraries were constructed using the TOPO TA Cloning kit (Invitrogen, Carlsbad, CA, USA). The amplified DNA fragments were ligated into the plasmid vector pCR®4-TOPO. The ligation products were subsequently transformed into One Shot TOP10 chemically competent *Escherichia coli* cells (Invitrogen, Carlsbad, CA, USA) according to the manufacturer's instructions. Transformants were randomly picked after incubation overnight at 37 °C and transferred to multi-well plates containing Luria–Bertani (LB) medium supplemented with 100 µg·mL⁻¹ ampicillin. Afterwards the plates were incubated overnight at the same temperature. Amplification of plasmids for confirming the presence of inserts was carried out using the primer pair M13/T7 (5'-CAGCAAACAGCTATGAC-3'/5'-TAATACGACTCACTATAGGG-3'). On average 100 clones from each library was sequenced by Macrogen Europe Sequencing Services (Amsterdam, The Netherlands) using the primers 27F for bacteria and ITS5 for fungi.

The clone sequences obtained in this study were deposited in GenBank under accession numbers LR216298–LR216639.

2.4.3. Sequence Comparisons and Phylogenetic Analysis

Bioinformatic tools were used to infer taxonomic classification. Sequences were aligned and checked for chimera by chimera.slayer implemented in the software package mothur [11]. Putative chimeric sequences were excluded from further analysis. Aligned sequences were clustered into operational taxonomic units (OTUs) using mothur, with a 97% sequence identity cutoff, and to generate the respective rarefaction curves at evolutionary distances of 3%, 5% and 20%. One clone for each OTU defined at 3% of distance (a rough approximation to species level) was chosen as representative and its sequence was submitted to GenBank. Taxonomic classification of each OTU and isolated bacterial strains was done by comparing the sequences to the non-redundant database of sequences at the National Center for Biotechnology Information (NCBI), using BLASTN (basic local alignment search tool) algorithm [12], and EzBiocloud database [13].

3. Results

3.1. Mineralogical Composition of Ceramic Raw Materials

The spectra obtained from samples 2B, 3C and 7G (Figure 2) are characterized by several peaks, with different intensity and sharp features: in the O–H stretching region a sharp peak at $\sim 3675\text{ cm}^{-1}$ which were assigned to the O–H stretching vibration of Mg_3OH group of talc minerals. A broad hump at $\sim 3400\text{ cm}^{-1}$ was assumed to be due to adsorbed atmospheric water. All the three spectra show sharper peaks around 1020, 677 and 470 cm^{-1} . The vibrational bands at 470 and 1020 cm^{-1} are ascribed to S–O–Si stretching vibrational bands, whereas the band at 677 cm^{-1} reflects the Si–O–Mg bond [14].

Sample 4D is mainly composed of kaolinite, with minor quantities of quartz (Figure 2). Quartz was identified by Si–O asymmetrical stretching vibration at 1087 cm^{-1} , Si–O symmetrical stretching vibration between $800\text{--}780\text{ cm}^{-1}$, Si–O symmetrical bending vibration at 696 cm^{-1} and Si–O asymmetrical bending vibration at 470 cm^{-1} . Kaolinite shows bands at 3695 and 3622 cm^{-1} ascribed to vibrations of the external and to the inner hydroxyl groups. In the 1000 cm^{-1} and 500 cm^{-1} region, the main functional groups are Si–O and Al–OH. The Al–OH absorption peak was identified at $891\text{--}915\text{ cm}^{-1}$. The band at 914 cm^{-1} corresponds to Al–OH bending vibrations of kaolinite, and the doublet at $780\text{--}798\text{ cm}^{-1}$ is related to Si–O–Si inter tetrahedral bridging bonds [15].

Sample 5E of bentonite shows absorption bands, with different intensities, at 3430, 2926, 2852, 1632, 1450, 1100, 1032, 918, 879, 782, 693, 530, 472, 430 cm^{-1} (Figure 2). A broad band at 3430 cm^{-1} is assigned to O–H stretching of structural hydroxyl groups and water present in the mineral. A very sharp and intense band observed at 1630 cm^{-1} is due to the asymmetric O–H stretch (deformation mode) of water and is a structural part of the mineral. Characteristic absorption of montmorillonite clay can be observed in the region between 1113 and 1032 cm^{-1} , characteristic of the Si–O bond, and between 918 and 782 cm^{-1} , corresponding to the octahedral layers of the aluminosilicate. The bands at 472 cm^{-1} and 430 cm^{-1} are attributed to the Si–O–Si deformation band [16].

The FTIR spectra of Sample 6F (Figure 2) confirmed the composition of this raw material, i.e., barium carbonate. A broad peak at 3427 cm^{-1} is observed and was assumed to be due to adsorbed atmospheric water. A strong peak at 1433 cm^{-1} is associated with asymmetric stretching vibrations of C–O bond at CO_3^{2-} . The absorption bands at 6923 cm^{-1} and 856 cm^{-1} are assigned to the bending out-of-plane vibrations and in-plane vibrations of O–C–O at CO_3^{2-} [17].

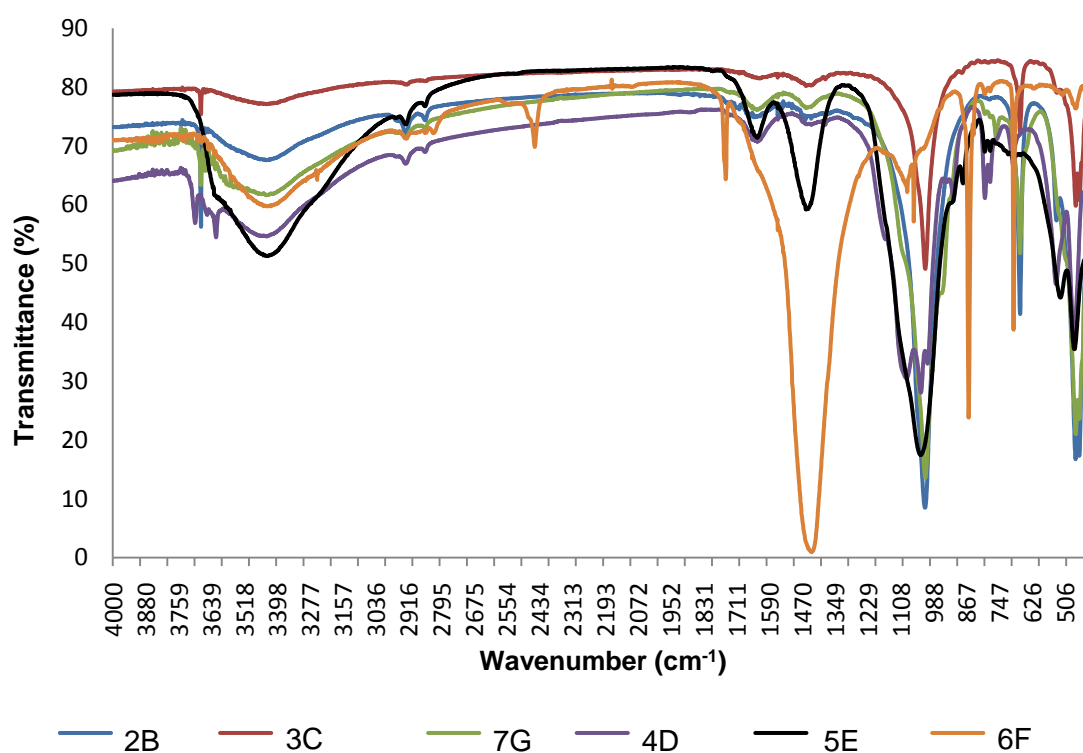


Figure 2. Fourier Transform Infrared spectra of the ceramic raw materials (Table 1) used by Rauschert Portuguesa.

3.2. Composition of Microbial Communities Associated with Ceramic Raw Materials

Bacterial 16S rRNA gene fragments were amplified from samples 1A, 2B, 4D, 6F, 7G and 8H, whereas fungal ITS gene fragments were solely amplified from sample 7G. Therefore, 16S rRNA gene fragment clone libraries were built for samples 1A, 2B, 4D, 6F, 7G and 8H, and a fungal ITS gene fragment clone library was built for sample 7G (hereinafter sample 7G-F) to identify the bacterial and fungal communities associated with ceramic raw materials used at Rauschert Portuguesa.

Analysis of the obtained 16S rRNA gene fragment sequences showed an abundance of bacteria from the phyla Proteobacteria and Actinobacteria in all samples (Figure 3), mainly represented by bacteria belonging to the orders Rhizobiales, Propionibacteriales, Pseudomonadales, Pseudonocardiales and Burkholderiales (Figure 3 and Tables S1–S6). Samples 1A (mill), 4D (clay), 7G (talc) and 8H (mixing tank) showed the highest bacterial diversity, with 28 genera identified in 7G, 23 genera in 8H and 20 genera in samples 1A and 4D (Figure 4 and Tables S1, S3, S5, S6).

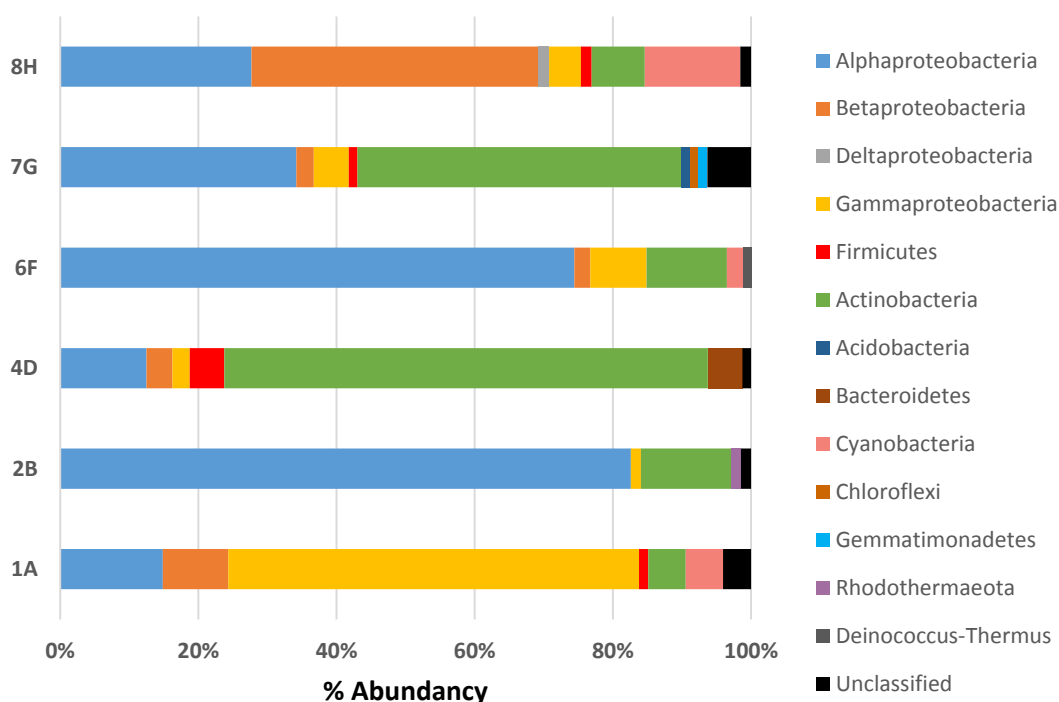


Figure 3. Distribution of bacterial phyla retrieved from samples 1A (mill ceramic suspension), 2B (talc 1), 4D (clay), 6F (barium carbonate), 7G (talc 3) and 8H (tank ceramic slip).

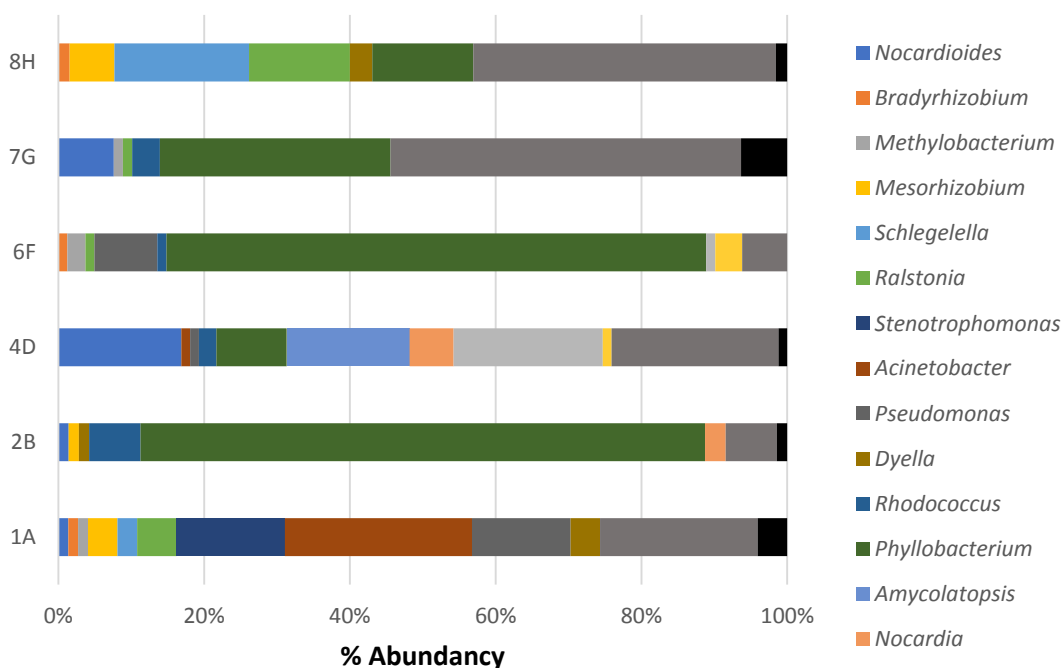


Figure 4. Distribution of bacterial genera retrieved from samples 1A (mill ceramic suspension), 2B (talc 1), 4D (clay), 6F (barium carbonate), 7G (talc 3) and 8H (tank ceramic slip).

Sample 1A was mainly dominated by the genera *Acinetobacter*, *Stenotrophomonas* and *Pseudomonas* (26%, 15% and 14%, respectively). Sample 4D was mainly represented by *Pseudonocardia* (21%), followed by *Amycolatopsis* (17%), *Nocardioiides* (17%) and *Phyllobacterium* (10%) (Figure 4). In sample 7G, the most predominant genera were *Phyllobacterium* (34%), *Gaiella* (8%) and *Streptomyces* (8%), with a high number of genera represented by only one bacterium (27%). In sample 8H, the most prevalent genera were *Schlegelella* (19%), *Ralstonia* and *Phyllobacterium* (14% each). Samples 2B (Talc 1) and 6F

(Barium carbonate) showed lower diversity of bacteria, with 9 and 13 genera identified, respectively. Sample 2B was almost completely dominated by bacteria belonging to the genus *Phyllobacterium* (80%). In Sample 6F, most of the identified bacteria were also represented by the same genus (70%) with a small representation of other genera such as *Pseudomonas* (8%) and *Nocardia* (6%).

The phylogenetic affiliations of the sequenced clones of samples 1A, 2B, 4D, 6F, 7G and 8H were also related to uncultured bacteria from a wide variety of isolation sources (Tables S1–S6), mainly from natural ambiances, such as marine environments, mines, ground waters, lakes, sediments from rivers and deep sea, air from a cave, lava tubes, rainwater, desert, periglacial environments, etc. The most frequent isolation sources of the closest matches were different types of soil (acid soils, contaminated soils, forest soil, alkaline saline soils, soil from a prairie, agricultural soil, grassland soil, soil of a glacier, permafrost soil, rice paddy soil, karst cave soil, etc.) and environments associated with roots of plants (rhizospheres) that are present in all samples. Interestingly, a substantial number of bacteria were isolated from biofilms from different materials: mineral substrates, waste ores, microplastics, concrete, limestone, basalt bedrock, rock of Etruscan tombs, polymetallic nodules and moonmilk speleothems (Tables S1–S6).

Analysis of the ITS gene fragment sequences, obtained from sample 7G–F, revealed 26 different genera from 9 orders (Figure 5 and Table S7). The great majority of sequences belong to the phylum Ascomycota (77% of total sequences), being *Penicillium* the most detected genus (19%) followed by *Hypocreales* and *Talaromyces* (17% both). Other fungi were also identified with smaller prevalence, belonging to the phyla Basidiomycota, represented by the genus *Scleroderma* (7%), and Muromycota, represented by *Mortierella* (7%).

In addition, the clone sequences obtained from sample 7G–F were analyzed taking into account the isolation sources of their closest relatives (Table S7). A high percentage of clones showed similarity to fungal clones isolated from root environments (rhizosphere soil, root mycobionts, washed and surface-sterilized roots, plant roots and mycorrhiza) being the most frequent isolation sources in this sample. Other isolation sources included extremely acidic soils, soil from an ancient tomb, alpine plants, living leaves and bryophyte crust, among others (Table S7). Interestingly, one DNA sequence obtained from sample 7G–F was phylogenetically affiliated to *Doratomyces* sp., which was isolated from a plasticized polyvinyl chloride (pPVC) (Table S7).

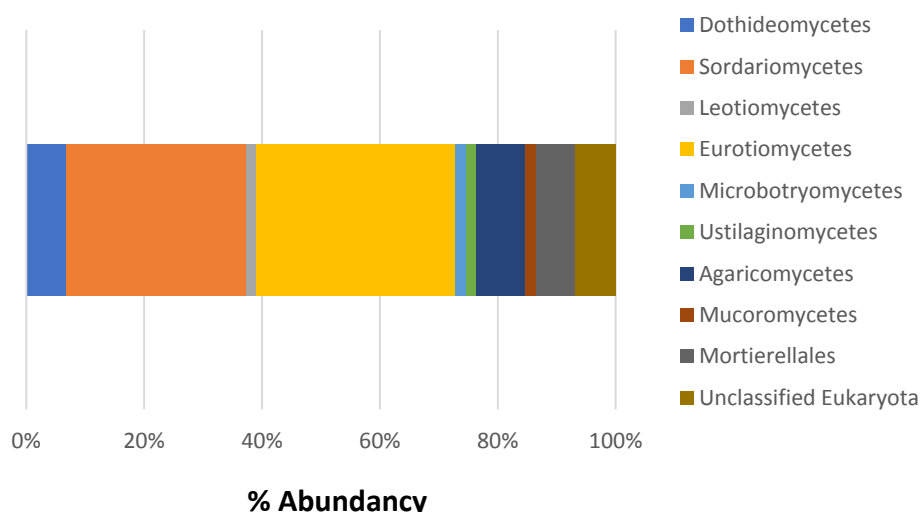


Figure 5. Phylogenetic affiliations (order level) of the ITS sequences obtained from sample 7G–F (talc 3).

Rarefaction curves showed that species richness for bacterial communities failed to reach a saturation phase at 3% and 5% of evolutionary distance in samples 1A, 2B, 4D, 7G and 8H (Figure S1). This suggests that further sequencing effort is required to detect additional phylotypes. However, enough clones were studied to reliably characterize the major microorganisms present in the ceramic

raw materials and slip. Only the rarefaction curve for the bacterial communities of sample 6H trended towards a plateau at genera level (Figure S1). For the fungal community in sample 7G–F, the rarefaction curve followed the same pattern as bacteria, even at 20% of evolutionary distance (data not shown).

3.3. Isolated Microorganisms

Bacteria and fungi were isolated from samples 1A, 2B, 3C, 4D, 7G and 8H collected at Rauschert Portuguesa. For samples 1A, 4D and 8H, 10-fold and 100-fold dilutions were performed to obtain isolated colonies.

Analysis of the 16S rRNA gene sequences of the isolated strains showed lower bacterial diversity (Table S8), in comparison with the biodiversity found by DNA-based analyses of the environmental samples (Tables S1–S6). In general, high percentages of similarity (between 99% and 100%) with the closest cultured relatives were found (Table S8). The majority of bacteria belong to the phyla Proteobacteria and Actinobacteria (Table S8), similarly to what was observed in the molecular biology approach. Samples 1A and 8H showed the greatest diversity, with 6 and 8 different genera identified, respectively. The most represented genus in sample 1A was *Hydrogenophaga* (45.5%), whereas *Microbacterium* (32%), *Pseudomonas* (21%) and *Acidovorax* (18%) were the dominant genera identified in sample 8H (Table S8). Samples 2B, 3C, 4D and 7G showed considerably less biodiversity. From sample 2B, bacterial strains belonging to four different genera were isolated, being *Glutamicibacter* (40%) the most prevalent (Table S8). Bacteria isolated from sample 3C belong to the genera *Bacillus* (67%) and *Arthrobacter* (33%). Notably, this was the only sample which was not dominated by Proteobacteria or Actinobacteria, being Firmicutes the most represented phylum (Table S8). From sample 4D, only three different genera were isolated: *Pseudomonas* (47%), *Arthrobacter* (43%), and *Microbacterium* (10%). In sample 7G, *Nocardioiodes* (67%) and *Herbaspirillum* (33%) were the identified genera.

The isolation sources of the closest relatives collected from the NCBI database (Table S8), showed the same trend as that observed for the microbial communities detected in the clone libraries. Natural environments, such as sediments, rhizosphere, contaminated soils and sandy soil, were the most frequent sources, as stated previously.

A total of 46 fungi were isolated from samples 1A, 2B, 3C and 7G (Table S9). Almost all the isolated fungi, identified by light microscopy, belong to the phylum Ascomycota (Figure 6, Table S9). As observed for the isolated bacteria, the diversity of fungi obtained by culture methods was lower than by molecular biology techniques. However, fungi were isolated from four samples (1A, 2B, 3C and 7G), instead of only one sample (7G). From sample 1A, only one strain of *Cladosporium* was isolated (Table S9). Eight different genera were isolated from samples 2B, 3C and 7G, being *Penicillium* (34%), *Monilia* (25%) and *Aspergillus* (13%) the most representative (Figure 6). Five different genera were isolated from sample 2B, being *Penicillium* (50%) and *Monilia* (20%) the most abundant. Sample 3C was represented by four different genera, being *Aspergillus* (40%) and *Rhizopus* (30%) the dominant genera identified. Finally, five different genera were isolated from sample 7G, mainly represented by *Penicillium* (40%) and *Rhizopus* (30%).

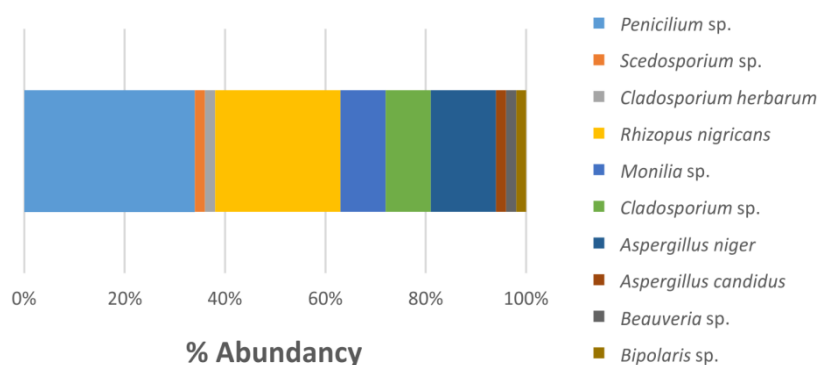


Figure 6. Identification of fungal strains isolated from samples 1A, 2B, 3C and 7G.

4. Discussion

The DNA-based analyses performed in this work for characterizing the microbial communities associated with ceramic raw materials and slips from Rauschert Portuguesa revealed that the prokaryotic community structure consisted mainly of phylotypes affiliated to Actinobacteria and Proteobacteria.

The significant abundance of bacteria from the phylum Proteobacteria might be associated with the chemical and mineralogical composition of the raw materials (clays and talcs), as both Alphaproteobacteria and Gammaproteobacteria have been frequently identified in soils rich in clay minerals, independently of their geographical location [18–20]. Alphaproteobacteria is a diverse class of Proteobacteria typically found in soils and marine environments, with many important biological roles. For instance, members of the genus *Sphingomonas* (reported in samples 1A and 8H) have been used for a wide range of biotechnological applications due to their biosynthetic capabilities [21]. They are able to produce the extracellular polymer gellan, which is a heteropolysaccharide composed of a unit of α -L-rhamnose, two β -D-glucoses and a β -D-glucuronate. This polymer easily forms stable gels at very low concentration, but the process is extremely dependent on certain properties such as pH, temperature and presence/type and concentration of gel promoting cations [21]. These gelation properties are extremely useful, especially in the food and pharmaceutical industries, where gellan gum is widely used as gelling agent [22]. The Gammaproteobacteria are a class of bacteria usually reported in polluted underground environments due to their great adaptability to changing environmental conditions [23,24]. These environments have been previously reported as an important source of exopolysaccharide-producing bacteria [25]. In fact, Gammaproteobacteria has been described as the most dominant group in wastewater-irrigated soils [26]. It is important to highlight that all of the samples studied in the present work are related to soil minerals. For example, talc is a type of clay mineral composed of hydrated magnesium silicate, and bentonite is an aluminum phyllosilicate composed mostly of montmorillonite. This is in agreement with the most common isolation sources of the closest recognized relatives listed in Tables S1–S6.

Other isolation sources of the closest uncultured clones and isolated microorganisms were roots and rhizosphere. A great number of bacteria dwelling in these environments are EPS producers and play an important role in influencing soil structure and physicochemical properties [27]. EPS also promote stabilization of soil aggregates and water regulation through plant roots, due to their unique water-retaining properties, enhancing plant growth [28,29].

Several clone sequences showed low similarity with their cultured closest relatives (Tables S1–S6) and could not be placed into an already described taxon. This suggests that affiliation to species-level could be questionable in some cases and that some of these sequences could represent novel species of bacteria. The generally accepted 16S similarity cutoff to identify and recognize new species is 98.7% [30], higher than the previous cutoff of 97.5% [31]. This means that a pairwise sequence similarity less than 98.7% does not guarantee a good identification to the species level. Thus, although 16S rRNA sequences can be used routinely to distinguish and establish relationships between genera and species, very recently diverged species may not be recognizable. Regarding our samples, several clones exhibited less than 98% or 97% sequence identity which suggests the existence of undescribed species, with no closely related sequences in current databases. It is also important to note that studies of microbial diversity based on conventional molecular biology techniques (PCR, cloning and Sanger sequencing) usually fail to cover all of the communities present in the samples and a deeper covering of them is frequently out of reach [32]. Hence, future research directions on the microbiome of ceramic raw materials should comprise next generation sequencing technologies to yield a near-complete coverage of the microbial communities naturally occurring in such materials and shed light on the mechanisms for EPS production.

Potential exopolysaccharide producers were identified in the studied samples. The alphaproteobacteria *Sphingomonas* sp., the gammaproteobacteria *Pseudomonas xanthomarina*, *Pseudomonas stutzeri*, *Pseudomonas koreensis* and *Acinetobacter lwoffii*, and the Firmicutes bacterium *Bacillus altitudinis*, detected in the clone libraries of sample 1A, are potential EPS producers, when the appropriate

growth conditions are settled. *Pseudomonas xanthomarina* is highly related to *Pseudomonas kunmingensis* and both have been studied for their exopolysaccharide-producing activity [33]. *Pseudomonas stutzeri* is a marine bacterium capable of producing EPS which could be used as functional-food components, together with their derivatives [34,35]. *Pseudomonas koreensis* is a biosurfactant-producing bacterium [36–38] with other interesting properties, such as solubilization of heavy metals [39] and lipase activity [40]. Members of the *Acinetobacter* genus have been extensively studied due to their production of bioemulsifiers and biosurfactants with tremendous applications in the petroleum, medicine and chemical industries, among others [41]. Specifically, *Acinetobacter lwoffii* shows great potential as bioemulsifier. In a study carried out by reference [42], who tested six *Acinetobacter* sp. isolated from human skin, the *Acinetobacter lwoffii* strain showed the maximum emulsification activity in the initial screening experiment and later exhibited the maximum bioemulsifier production. *Bacillus altitudinis* synthesizes a heteropolysaccharide with antitumor, antioxidant and antimicrobial activities [43].

Two sequences from the clone library of sample 1A showed similarity with the genus *Micrococcus* sp. which is capable of synthesizing exopolysaccharides [44] but, to our knowledge, no study has focused on its EPS production yet.

In the clone library from sample 4D, two clones reached 95–98% of similarity with the sulfur oxidizing betaproteobacterium *Thiobacillus thioparus*. This bacterium usually appears in close contact with metal surfaces in industrial environments and its EPS composition varies according to growth conditions [45]. In the clone library from sample 6F, only the detected betaproteobacterium *Aquabacterium commune* has been related to biofilm formation, frequently detected on drinking water distribution systems [46]. Finally, two clones from sample 8H showed similarity with the bacteria *Streptococcus sanguinis* (98%) and *Acidovorax soli* (99%), both species known by their capability to form biofilms in different environments [47,48].

Among the isolated bacteria, several strains are potential EPS producers. Four strains isolated from samples 1A and 8H showed affiliation with *Pseudomonas stutzeri* [34,35] and one strain from sample 2B with *Kocuria rosea*. This latter is a halophilic bacterium able to produce a polysaccharide designated as Kocuran [49]. Recent publications claim that certain strains of *Kocuria rosea* have great potential to be exploited as a source of EPSs utilized in industry, as well as in the biotreatment of hypersaline environments [50]. In addition, the genus *Brachybacterium* was detected in the isolates of sample 1A with a 100% rate of similarity, represented by the species *Brachybacterium rhamnsum*. These microorganisms are known for producing EPS such as levan [25]. Levan is a β -(2,6)-linked fructose polymer with a remarkably low intrinsic viscosity, offering a broader spectrum of biotechnological applications. In fact, this polymer can be produced extracellularly by numerous bacteria, including the genera *Acetobacter*, *Bacillus*, *Erwinia*, *Gluconobacter*, *Halomonas*, *Microbacterium*, *Pseudomonas*, *Streptococcus* and *Zymomonas* [51]. Levan as a biofilm component of soil bacterial species contributes to shield bacterial cells from desiccation, to glue cells and to protect the community from predatory organisms. It also serves as an extracellular nutrient reservoir that can be used as an energy source by bacteria under starvation conditions [51]. Many applications for levan have been reported in the literature, which are particularly related to its capacity to form thin films for medical uses or for bio-based food packaging films [52]. Levan-based films are clear, flexible and good oxygen barriers when mixed with the clay montmorillonite [53].

In samples 1A and 3C, two isolates had the bacterium *Bacillus aryabhatai* as their closest match to known isolates (100% and 99% of similarity, respectively), whose capacity of producing EPS has been tested previously in a study carried out by reference [54]. These authors recorded the highest EPS dry weight for this species respect to other halotolerant strains. Moreover, in sample 4D one isolated bacteria was affiliated to the species *Arthrobacter sulfonivorans* (98%), an actinobacteria whose capacity of producing EPS has been previously reported [55]. Finally, two alphaproteobacteria with the capacity of synthesizing EPS were isolated exclusively from sample 8H: *Brevundimonas diminuta* [56] and *Rhizobium radiobacter* [57].

No potential EPS producing fungi were isolated from the samples collected in Rauschert Portuguesa. However, four fungi potentially able to produce EPS were identified in the clone libraries from sample 7G–F: *Penicillium citrinum*, which synthesize a malonylated polysaccharide called malonogalactan [58], *Fusarium oxysporum* [59], *Acremonium persicinum* [60], which is also used for β -glucanases production [61], and the yeast *Rhodotorula mucilaginosa* [62]. The exopolysaccharide produced by the latter possesses antimicrobial and antibiofilm properties and therefore could have potential applications to inhibit microbial colonization in medical and industrial settlings [63]. Several fungal orders were also detected in sample 7G–F which have been previously reported as EPS synthesizers, such as *Hypocreales* [64] and *Diaporthales* [65]. The most common fungal exopolysaccharide used in the industry is pullulan. This is a linear glucosic homopolysaccharide, excreted by the non-toxic and non-pathogen fungus *Aureobasidium pullulans* [66]. As an odorless and non-toxic white colored powder, pullulan is easily soluble in water providing clear and viscous solutions due to its structural flexibility. This polymer also has high adhesion, sticking, lubrication and film forming abilities [67]. These properties are of utmost interest for the industrial ceramic to improve the rheological properties of the slips and to decrease the difficulties observed during the dry pressing process. In Figure 7, we summarize the potential effect of the application of EPS to the ceramic materials and its impact on the ceramic rheological properties. Based in the literature, it is hypothesized that EPS, such as pullulan, gellan or xanthan gum, may improve the viscosity of the slips and the performance of in terms of adhesion and flexural strength of the conformed bodies.

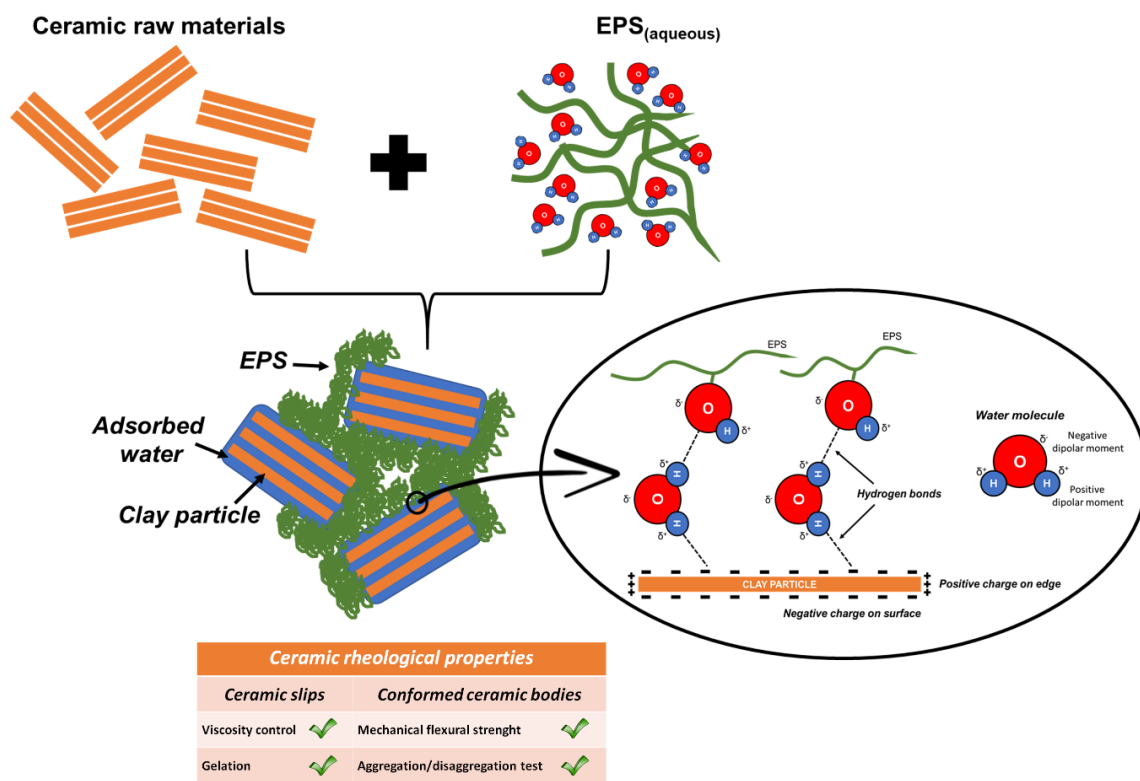


Figure 7. Conceptual model of the effect of adding EPS to ceramic materials and their potential impact on the rheological properties.

5. Conclusions

The colonization pattern from all the samples revealed the presence of microorganisms that are usually present in natural environments, particularly in clay soils. Hence, the identified bacteria and fungi in all samples are in fair agreement with the nature of the raw materials used in the preparation of the ceramic slips (clays and talcs).

The approach used allowed us to obtain a general view of the microbial community composition of the ceramic raw materials and slips and revealed consistent results among culture-dependent and -independent techniques. Both methods can be used in a complementary way, although culture techniques may be less sensitive than molecular biology.

The analysis of the microbial communities present in the raw materials and ceramic suspensions from the industrial process at Rauschert Portuguesa allowed us to detect some potential EPS producers, both bacteria and fungi, in these samples. The most interesting microorganisms detected were *Sphingomonas* sp., *Pseudomonas xanthomarina*, *Pseudomonas stutzeri*, *Pseudomonas koreensis*, *Acinetobacter lwoffii*, *Penicillium citrinum*, *Fusarium oxysporum*, *Acremonium persicinum* and *Rhodotorula mucilaginosa*, all of them with the ability of synthesize exopolysaccharides when the appropriate conditions are settled.

The EPS producers found among the identified microorganisms open the door to future studies focused on EPS production and application to the ceramic production process for improving the rheological properties of the final ceramic components. In addition, microbial biopolymers represent eco-friendly and cost-effective alternatives to the conventional synthetic additives currently used in the ceramic industry.

Supplementary Materials: The following are available online at <http://www.mdpi.com/2075-163X/9/5/316/s1>, Figure S1: Rarefaction curves, Table S1: Phylogenetic affiliations of the 16S rRNA gene sequences of total bacteria obtained from sample 1A (74 sequences, 64 OTUs), Table S2: Phylogenetic affiliations of the 16S rRNA gene sequences of total bacteria obtained from sample 2B (69 sequences, 51 OTUs), Table S3: Phylogenetic affiliations of the 16S rRNA gene sequences of total bacteria obtained from sample 4D (80 sequences, 54 OTUs), Table S4: Phylogenetic affiliations of the 16S rRNA gene sequences of total bacteria obtained from sample 6F (86 sequences, 38 OTUs), Table S5: Phylogenetic affiliations of the 16S rRNA gene sequences of total bacteria obtained from sample 7G (79 sequences, 48 OTUs), Table S6: Phylogenetic affiliations of the 16S rRNA gene sequences of total bacteria obtained from sample 8H (65 sequences, 38 OTUs), Table S7: Phylogenetic affiliations of the OTUs obtained from the ITS fungal sequences of sample 7G–F, Table S8: Phylogenetic affiliations of the bacterial strains isolated from samples 1A, 2B, 3C, 4D, 7G and 8H, Table S9: Taxonomy of fungi isolated from samples 1A, 2B, 3C and 7G.

Author Contributions: Conceptualization, D.D., O.N., A.D. and A.Z.M.; Formal analysis, A.M.G.-S., B.M.-M. and M.F.; Funding acquisition, A.Z.M.; Investigation, A.D. and A.Z.M.; Project administration, O.N.; Resources, D.D.; Supervision, M.F., R.S., S.M. and A.Z.M.; Validation, D.D.; Writing—original draft, A.M.G.-S. and B.M.-M.; Writing—review & editing, D.D., O.N., A.D. and A.Z.M.

Funding: This research was funded by *Fundação para a Ciência e a Tecnologia*, project EXPL/CTM-CER/0637/2012.

Acknowledgments: The authors acknowledge Rauschert Portuguesa, S.A., for cooperation and knowledge.

Conflicts of Interest: The authors declare no conflict of interest. The funders had no role in the design of the study; in the collection, analyses, or interpretation of data; in the writing of the manuscript, or in the decision to publish the results.

References

1. Evans, J.R.G. Seventy ways to make ceramics. *J. Eur. Ceram. Soc.* **2008**, *28*, 1421–1432. [[CrossRef](#)]
2. Flemming, H.C.; Wingender, J. Relevance of microbial extracellular polymeric substances (EPSs)-Part II: Technical aspects. *Water Sci. Technol.* **2001**, *43*, 9–16. [[CrossRef](#)]
3. Ates, O. Systems biology of microbial exopolysaccharides production. *Front. Bioeng. Biotechnol.* **2015**, *3*, 200. [[CrossRef](#)] [[PubMed](#)]
4. Moscovici, M. Present and future medical applications of microbial exopolysaccharides. *Front. Microbiol.* **2015**, *6*, 1012. [[CrossRef](#)] [[PubMed](#)]
5. Castillo, N.A.; Valdez, A.L.; Fariña, J.I. Microbial production of scleroglucan and downstream processing. *Front. Microbiol.* **2015**, *15*, 1106. [[CrossRef](#)] [[PubMed](#)]
6. Russo, P.; de Chiara, M.L.V.; Capozzi, V.; Arena, M.P.; Amodio, M.L.; Rascòn, A.; Dueñas, M.T.; Lòpez, P.; Spano, G. *Lactobacillus plantarum* strains for multifunctional oat-based foods. *Food Sci. Technol.* **2016**, *68*, 288–294. [[CrossRef](#)]
7. Ripari, V. Techno-functional role of exopolysaccharides in cereal-based, yogurt-like beverages. *Beverages* **2019**, *5*, 16. [[CrossRef](#)]

8. Frank, J.A.; Reich, C.I.; Sharma, S.; Weisbaum, J.S.; Wilson, B.A.; Olsen, G.J. Critical evaluation of two primers commonly used for amplification of bacterial 16S rRNA genes. *Appl. Environ. Microb.* **2008**, *74*, 2461–2470. [[CrossRef](#)] [[PubMed](#)]
9. Schabereiter-Gurtner, C.; Lubitz, W.; Rölleke, S. Application of broad-range 16S rRNA PCR amplification and DGGE fingerprinting for detection of tick-infecting bacteria. *J. Microbiol. Methods* **2003**, *52*, 251–260. [[CrossRef](#)]
10. White, T.J.; Bruns, T.; Lee, S.; Taylor, J. Amplification and direct sequencing of fungal ribosomal RNA genes for phylogenetics. In *PCR Protocols, A Guide to Methods and Applications*; Innis, M.A., Gelfand, D.H., Sninsky, J.J., White, T.J., Eds.; Academic Press: New York, NY, USA, 1990; pp. 315–322.
11. Schloss, P.C.; Westcott, S.L.; Ryabin, T.; Hall, J.R.; Hartmann, M.; Hollister, E.B.; Lesniewski, R.A.; Oakley, B.B.; Parks, D.H.; Robinson, C.J.; et al. Introducing mothur: Open source, platform-independent, community-supported software for describing and comparing microbial communities. *Appl. Environ. Microb.* **2009**, *75*, 7537–7541. [[CrossRef](#)]
12. Altschul, S.; Gish, W.; Miller, W.; Myers, E.; Lipman, D. Basic local alignment search tool. *J. Mol. Biol.* **1990**, *215*, 403–410. [[CrossRef](#)]
13. Yoon, S.H.; Ha, S.M.; Kwon, S.; Lim, J.; Kim, Y.; Seo, H.; Chun, J. Introducing EzBioCloud: A taxonomically united database of 16S rRNA gene sequences and whole-genome assemblies. *Int. J. Syst. Evol. Microbiol.* **2017**, *67*, 1613–1617. [[PubMed](#)]
14. Lagadic, L.; Mitchell, M.K.; Payne, B.D. Highly effective adsorption of heavy metal ions by a thiol-functionalized magnesium phyllosilicate clay. *Environ. Sci. Technol.* **2001**, *35*, 84–90. [[CrossRef](#)]
15. Saikia, B.; Parthasarathy, G. Fourier transform infrared spectroscopic characterization of kaolinite from Assam and Meghalaya, Northeastern India. *J. Mod. Phys.* **2010**, *1*, 206–210. [[CrossRef](#)]
16. Reddy, T.R.; Kaneko, S.; Endo, T.; Reddy, S.L. Spectroscopic characterization of bentonite. *J. Laser Opt. Photonics* **2017**, *4*, 171.
17. Sabet, M.; Salavati-Niasari, M.; Asgari Fard, Z. Synthesis and characterization of barium carbonate nanostructures via simple hydrothermal method. *Synth. React. Inorg. M.* **2016**, *46*, 317–322. [[CrossRef](#)]
18. Janssen, P.H. Identifying the Dominant Soil Bacterial Taxa in Libraries of 16S rRNA and 16S rRNA Genes. *Appl. Environ. Microb.* **2006**, *72*, 1719–1728. [[CrossRef](#)]
19. Labbé, D.; Margesin, R.; Schinner, F.; Whyte, L.G.; Greer, C.W. Comparative phylogenetic analysis of microbial communities in pristine and hydrocarbon-contaminated Alpine soils. *FEMS Microbiol. Ecol.* **2007**, *59*, 466–475. [[CrossRef](#)] [[PubMed](#)]
20. Niepceron, M.; Martin-Laurent, F.; Crampon, M.; Portet-Koltalo, F.; Akpa-Vinceslas, M.; Legras, M.; Bru, D.; Bureau, F.; Bodilis, J. GammaProteobacteria as a potential bioindicator of a multiple contamination by polycyclic aromatic hydrocarbons (PAHs) in agricultural soils. *Environ. Pollut.* **2013**, *180*, 199–205. [[CrossRef](#)]
21. Das, N.; Tripathi, N.; Basu, S.; Bose, C.; Maitra, S.; Khurana, S. Progress in the development of gelling agents for improved culturability of microorganisms. *Front. Microbiol.* **2015**, *6*, 698. [[CrossRef](#)]
22. Osmalek, T.; Froelich, A.; Tasarek, S. Application of gellan gum in pharmacy and medicine. *Int. J. Pharm.* **2014**, *466*, 328–340. [[CrossRef](#)]
23. Miller, A.Z.; Hernández-Mariné, M.; Jurado, V.; Dionísio, A.; Barquinha, P.; Fortunato, E.; Afonso, M.J.; Chaminé, H.I.; Saiz-Jimenez, C. Enigmatic reticulated filaments in subsurface granite. *Env. Microbiol. Rep.* **2012**, *4*, 596–603. [[CrossRef](#)] [[PubMed](#)]
24. Miller, A.Z.; Garcia-Sanchez, A.M.; Martin-Sanchez, P.M.; Pereira, M.F.C.; Spangenberg, J.E.; Jurado, V.; Dionísio, A.; Afonso, M.J.; Chaminé, H.I.; Hermosin, B.; et al. Origin of abundant moonmilk deposits in a subsurface granitic environment. *Sedimentology* **2018**, *65*, 1482–1503. [[CrossRef](#)]
25. Djuric, A.; Gojic-Cvijovic, G.; Jakovljevic, D.; Kekez, B.; Kojic, J.S.; Mattinen, M.L.; Harju, I.E.; Vrvic, M.M.; Beskoski, V.P. *Brachybacterium* sp. CH-KOV3 isolated from an oil-polluted environment—A new producer of levan. *Int. J. Biol. Macromol.* **2017**, *104*, 311–321. [[CrossRef](#)]
26. Broszat, M.; Nacke, H.; Blasi, R.; Siebe, C.; Huebner, J.; Daniel, R.; Grohmann, E. Wastewater irrigation increases the abundance of potentially harmful Gammaproteobacteria in soils in Mezquital Valley, Mexico. *Appl. Environ. Microb.* **2014**, *80*, 5282–5291. [[CrossRef](#)] [[PubMed](#)]

27. Paul, S.; Dukare, A.S.; Bandeppa; Manjunatha, B.S.; Annapurna, K. Plant growth-promoting rhizobacteria for abiotic stress alleviation in crops. In *Advances in Soil Microbiology: Recent Trends and Future Prospects. Microorganisms for Sustainability*; Adhya, T., Mishra, B., Annapurna, K., Verma, D., Kumar, U., Eds.; Springer: Singapore, 2017; Volume 4.
28. Roberson, E.B.; Firestone, M.K. Relationship between desiccation and exopolysaccharide production in a soil *Pseudomonas* spp. *Appl. Environ. Microb.* **1992**, *58*, 1284–1291.
29. Kaushal, M.; Wani, S.P. Plant-growth-promoting rhizobacteria: Drought stress alleviators to ameliorate crop production in drylands. *Ann. Microbiol.* **2016**, *66*, 35–42. [[CrossRef](#)]
30. Chun, J.; Oren, A.; Ventosa, A.; Christensen, H.; Arahal, D.; da Costa, M.; Rooney, A.; Yi, H.; Xu, X.; De Meyer, S.; et al. Proposed minimal standards for the use of genome data for the taxonomy of prokaryotes. *Int. J. Syst. Evol. Microbiol.* **2018**, *68*, 461–466. [[CrossRef](#)]
31. Fox, G.E.; Wisotzkey, J.D.; Jurtshuk, P., Jr. How close is close: 16s rRNA sequence identity may not be sufficient to guarantee species identity. *Int. J. Syst. Bacteriol.* **1992**, *42*, 166–170. [[CrossRef](#)] [[PubMed](#)]
32. Bent, S.J.; Forney, L.J. The tragedy of the uncommon: Understanding limitations in the analysis of microbial diversity. *ISME J.* **2008**, *2*, 689–695. [[CrossRef](#)] [[PubMed](#)]
33. Xie, F.H.; Ma, S.; Quan, D.; Liu, G.; Chao, C.Y.; Qian, S. *Pseudomonas kunmingensis* sp. nov., an exopolysaccharide-producing bacterium isolated from a phosphate mine. *Int. J. Syst. Evol. Microbiol.* **2014**, *64*, 559–564. [[CrossRef](#)] [[PubMed](#)]
34. Maalej, H.; Boisset, C.; Hmidet, N.; Buon, L.; Heyraud, A.; Nasri, M. Purification and structural data of a highly substituted exopolysaccharide from *Pseudomonas stutzeri* AS22. *Carbohydr. Polym.* **2014**, *112*, 404–411. [[CrossRef](#)] [[PubMed](#)]
35. Wu, S.; Zheng, R.; Sha, Z.; Sun, C. Genome Sequence of *Pseudomonas stutzeri* 273 and Identification of the Exopolysaccharide EPS273 Biosynthesis Locus. *Mar. Drugs* **2017**, *15*, 218. [[CrossRef](#)] [[PubMed](#)]
36. Hultberg, M.; Bengtsson, T.; Liljeroth, E. Late blight on potato is suppressed by the biosurfactant-producing strain *Pseudomonas koreensis* 2.74 and its biosurfactant. *Biocontrol* **2010**, *55*, 543–550. [[CrossRef](#)]
37. Hultberg, M.; Alsberg, T.; Khalil, S.; Alsanius, B. Suppression of disease in tomato infected by *Pythium ultimum* with a biosurfactant produced by *Pseudomonas koreensis*. *Biocontrol* **2010**, *55*, 435–444. [[CrossRef](#)]
38. Toribio, J.; Escalante, A.E.; Caballero-Mellado, J.; González-González, A.; Zavala, S.; Souza, V.; Soberón-Chávez, G. Characterization of a novel biosurfactant producing *Pseudomonas koreensis* lineage that is endemic to Cuatro Ciénegas Basin. *Syst. Appl. Microbiol.* **2011**, *34*, 531–535. [[CrossRef](#)] [[PubMed](#)]
39. Babu, A.G.; Shea, P.J.; Sudhakaralk-BooJung, D.; Oh, B.T. Potential use of *Pseudomonas koreensis* AGB-1 in association with *Miscanthus sinensis* to remediate heavy metal(loid)-contaminated mining site soil. *J. Environ. Manag.* **2015**, *151*, 160–166. [[CrossRef](#)]
40. Anbu, P. Characterization of an extracellular lipase by *Pseudomonas koreensis* BK-L07 isolated from soil. *Prep. Biochem. Biotech.* **2014**, *44*, 266–280. [[CrossRef](#)]
41. Mujumdar, S.; Joshi, P.; Karve, N. Production, characterization, and applications of bioemulsifiers (BE) and biosurfactants (BS) produced by *Acinetobacter* spp.: A review. *J. Basic Microb.* **2019**, *59*, 277–287. [[CrossRef](#)]
42. Jagtap, S.; Yavankar, S.; Pardesi, K.; Chopade, B. Production of bioemulsifier by *Acinetobacter* species isolated from healthy human skin. *Indian J. Exp. Biol.* **2010**, *48*, 70–76.
43. Mohamed, S.S.; Amer, S.K.; Selim, M.S.; Rifaat, H.M. Characterization and applications of exopolysaccharide produced by marine *Bacillus altitudinis* MSH2014 from Ras Mohamed, Sinai, Egypt. *Egypt. J. Basic Appl. Sci.* **2018**, *5*, 204–209. [[CrossRef](#)]
44. Kiliç, N.K.; Dönmez, G. Environmental conditions affecting exopolysaccharide production by *Pseudomonas aeruginosa*, *Micrococcus* sp., and *Ochrobactrum* sp. *J. Hazard Mater.* **2008**, *154*, 1019–1024. [[CrossRef](#)] [[PubMed](#)]
45. Boretska, M.; Bellenberg, S.; Moshynets, O.; Pokhonenko, I.; Sand, W. Change of extracellular polymeric substances composition of *Thiobacillus thiooparus* in presence of sulfur and steel. *J. Microb. Biochem. Technol.* **2013**, *5*, 68–73. [[CrossRef](#)]
46. Ojeda, J.J.; Romero-González, M.E.; Banwart, S.A. Analysis of bacteria on steel surfaces using reflectance Micro-Fourier Transform Infrared Spectroscopy. *Anal. Chem.* **2009**, *81*, 6467–6473. [[CrossRef](#)]
47. Ge, X.; Kitten, T.; Chen, Z.; Lee, S.P.; Munro, C.L.; Xu, P. Identification of *Streptococcus sanguinis* genes required for biofilm formation and examination of their role in endocarditis virulence. *Infect. Immun.* **2008**, *76*, 2551–2559. [[CrossRef](#)] [[PubMed](#)]

48. Belgini, D.R.B.; Dias, R.S.; Siqueira, V.M.; Valadares, L.A.B.; Albanese, J.M.; Souza, R.S.; Torres, A.P.R.; Sousa, M.P.; Silva, C.C.; De Paula, S.O.; et al. Culturable bacterial diversity from a feed water of a reverse osmosis system, evaluation of biofilm formation and biocontrol using phages. *World J. Microb. Biotechnol.* **2014**, *30*, 2689–2700. [[CrossRef](#)]
49. Kumar, C.G.; Sujitha, P. Kocuran, an exopolysaccharide isolated from *Kocuria rosea* strain BS-1 and evaluation of its in vitro immunosuppression activities. *Enzyme Microb. Technol.* **2014**, *55*, 113–120. [[CrossRef](#)] [[PubMed](#)]
50. Gu, D.; Jiao, Y.; Wu, J.; Liu, Z.; Chen, Q. Optimization of EPS production and characterization by a halophilic bacterium, *Kocuria rosea* ZJUQH from Chaka Salt Lake with response surface methodology. *Molecules* **2017**, *22*, 814. [[CrossRef](#)] [[PubMed](#)]
51. Öner, E.T.; Hernández, L.; Combie, J. Review of Levan polysaccharide: From a century of past experiences to future prospects. *Biotechnol. Adv.* **2016**, *34*, 827–844. [[CrossRef](#)]
52. Costa, R.R.; Neto, A.I.; Calgeris, I.; Correia, C.R.; Pinho, A.C.M.; Fonseca, J.; Toksoy Öner, E.; Mano, J.F. Adhesive nanostructured multilayer films using a bacterial exopolysaccharide for biomedical applications. *J. Mater. Chem.* **2013**, *1*, 2367–2374. [[CrossRef](#)]
53. Chen, X.; Gao, H.; Ploehn, H.J. Montmorillonite-levan nanocomposites with improved thermal and mechanical properties. *Carbohydr. Polym.* **2014**, *101*, 565–573. [[CrossRef](#)]
54. Hong, B.H.; Joe, M.M.; Selvakumar, G.; Kim, K.Y.; Choi, J.H.; Sa, T.M. Influence of salinity variations on exocellular polysaccharide production, biofilm formation and flocculation in halotolerant bacteria. *J. Environ. Biol.* **2017**, *38*, 657–664. [[CrossRef](#)]
55. Ruzsnyák, A.; Akob, D.M.; Nietzsche, S.; Eusterhues, K.; Totsche, K.U.; Neu, T.R.; Frosch, T.; Popp, J.; Keiner, R.; Geletneky, J.; et al. Calcite biomineralization by bacterial isolates from the recently discovered pristine karstic herrenberg cave. *Appl. Environ. Microb.* **2012**, *78*, 1157–1167. [[CrossRef](#)]
56. Badireddy, A.R.; Chellam, S.; Yanina, S.; Gassman, P.; Rosso, K.M. Bismuth dimercaptopropanol (BisBAL) inhibits the expression of extracellular polysaccharides and proteins by *Brevundimonas diminuta*: Implications for membrane microfiltration. *Biotechnol. Bioeng.* **2008**, *99*, 634–643. [[CrossRef](#)]
57. Zhou, F.; Wu, Z.; Jin Han, C.C.; Ai, L.; Guo, B. Exopolysaccharides produced by *Rhizobium radiobacter* S10 in whey and their rheological properties. *Food Hydrocolloids* **2014**, *36*, 362–368. [[CrossRef](#)]
58. Kohama, T.; Fujimoto, M.; Kuninaka, A.; Yoshino, H. Structure of malonogalactan, an acidic polysaccharide of *Penicillium citrinum*. *Agric. Biol. Chem.* **1974**, *38*, 127–134.
59. Guo, S.; Mao, W.; Li, Y.; Tian, J.; Xu, J. Structural elucidation of the exopolysaccharide produced by fungus *Fusarium oxysporum* Y24-2. *Carbohydr. Res.* **2013**, *365*, 9–13. [[CrossRef](#)]
60. Seviour, R.J.; Stasinopoulos, S.J.; Auer, D.P.F.; Gibbs, P.A. Production of pullulan and other exopolysaccharides by filamentous fungi. *Crit. Rev. Biotechnol.* **1992**, *12*, 279–298. [[CrossRef](#)]
61. Pitson, S.M.; Seviour, R.J.; McDougall, B.M. Effect of carbon source on extracellular (1 → 3)- and (1 → 6)- β -glucanase production by *Acremonium persicinum*. *Can. J. Microbiol.* **1997**, *43*, 432–439. [[CrossRef](#)]
62. Takita, J.; Katohda, S.; Sugiyama, H. Structural determination of an exocellular mannan from *Rhodotorula mucilaginosa* YR-2 using ab initio assignment of proton and carbon NMR spectra. *Carbohydr. Res.* **2001**, *335*, 133–139. [[CrossRef](#)]
63. Vazquez-Rodriguez, A.; Vasto-Anzaldo, X.G.; Barboza Perez, D.; Vázquez-Garza, E.; Chapoy-Villanueva, H.; García-Rivas, G.; Garza-Cervantes, J.A.; Gómez-Lugo, J.J.; Gomez-Loredo, A.E.; Garza Gonzalez, M.T.; et al. Microbial competition of *Rhodotorula mucilaginosa* UANL-001L and *E. coli* increase biosynthesis of non-toxic exopolysaccharide with applications as a wide-spectrum antimicrobial. *Sci. Rep.* **2018**, *8*, 798. [[CrossRef](#)] [[PubMed](#)]
64. Yeh, C.W.; Zang, C.Z.; Lin, C.C.; Kan, S.C.; Chang, W.F.; Shieh, C.J.; Liu, Y.C. Quantitative and morphologic analysis on exopolysaccharide and biomass production from a truffle endophytic fungus *Hypocreales* sp. NCHU01. *J. Taiwan Inst. Chem. Eng.* **2014**, *45*, 108–114. [[CrossRef](#)]
65. Orlandelli, R.C.; Vasconcelos, A.F.D.; Azevedo, J.L.; Corradi da Silva, M.L.; Pamphile, J.A. Screening of endophytic sources of exopolysaccharides: Preliminary characterization of crude exopolysaccharide produced by submerged culture of *Diaporthe* sp. JF766998 under different cultivation time. *Biochim. Open* **2016**, *2*, 33–40. [[CrossRef](#)] [[PubMed](#)]

66. Leathers, T.D. Biotechnological production and applications of pullulan. *Appl. Microbiol. Biotechnol.* **2003**, *62*, 468–473. [[CrossRef](#)] [[PubMed](#)]
67. Singh, R.S.; Sainia, G.K.; Kennedy, J.F. Pullulan: Microbial sources, production and applications. *Carbohydr. Polym.* **2008**, *4*, 515–531. [[CrossRef](#)] [[PubMed](#)]



© 2019 by the authors. Licensee MDPI, Basel, Switzerland. This article is an open access article distributed under the terms and conditions of the Creative Commons Attribution (CC BY) license (<http://creativecommons.org/licenses/by/4.0/>).